Progress In Electromagnetics Research C, Vol. 74, 101–109, 2017

Wideband RCS Reduction of Vivaldi Antenna Based on Substrate Integrated Waveguide

Jing-Jing Xue[1], Wen Jiang[1, *], Shu-Xi Gong[1], and Sheng-Hui Zhang[2]

Abstract—A novel design for radar cross section (RCS) reduction of a bilateral Vivaldi antenna is presented. The method for RCS reduction is based on the wave-guiding characteristic of the substrate integrated waveguide (SIW) structure, which guides the incident energy to the lateral side of antenna plane. The bistatic RCS is controlled under the premise of reducing the monostatic RCS. Compared with the reference antenna, a significant monostatic RCS reduction is achieved over a wide frequency band ranging from 5 GHz to 12 GHz, and a remarkable monostatic RCS reduction at 7 GHz is as much as 34.73 dB without obvious radiation performance degradation. To verify the proposed strategy, prototypes of the reference and proposed antennas have been fabricated and measured. Good agreements between the simulated and measured results demonstrate that the proposed method preserves the radiation performances well and achieves an outstanding wideband RCS reduction.

1. INTRODUCTION

With the rapid development of the advanced detection and stealth technology, extensive attention on the radar cross section (RCS) reduction of different platforms has been paid due to the urgent requirement for defence application. As an indispensable device for communication systems, the antenna must transmit and receive electromagnetic wave effectively. Therefore, reducing the RCS of antennas is so difficult because the optimization of the scattering features would degrade the radiation performance of antennas. In recent years, many methods have been proposed to reduce the RCS of antennas since the antennas are the dominant scatterers for low-observable platforms [1]. In order to reduce the RCS of antennas, the system complexity will usually be increased and the radiation property of the antenna also may be affected. Various approaches have been raised to reduce the scattering signature of a stealth object, such as shaping the target [2, 3], coating with radar absorbing material (RAM) [4–6] and using the passive and active cancellation technology [7–9]. Recently, polarization conversion surfaces are utilized to design low RCS surface and antennas [10, 11], achieving a remarkable result in a wideband range.

Among the ultra-wide band (UWB) antennas, Vivaldi antennas [12, 13] are widely utilized in fire control systems which are installed in front of the aircraft because of the high gain, broad bandwidth and compact size. Hence, reducing the RCS of the UWB antenna is of great significance, especially covering the operation band. However, it is difficult to find a balance between the scattering characteristics and radiation performance by using conventional approaches. In [14], the RCS reduction of a dual-index Vivaldi antenna is investigated over a wide frequency band with the radiation performance almost unaffected. A phase-switched screen (PSS) is introduced in [15], but the RCS reduction of the antenna is obtained only at some frequency band. In [16], the modified metal radiator and the photonic band gap (PBG) structure are combined to reduce the RCS of Vivaldi antenna. For antipodal Vivaldi Antenna,

Received 12 February 2017, Accepted 10 May 2017, Scheduled 22 May 2017

* Corresponding author: Wen Jiang (jw13@vip.qq.com).

[1] National Key Laboratory of Antennas and Microwave Technology, Xidian University Xi'an, Shaanxi 710071, China. [2] Space Star Technology Co. Ltd, Beijing 100086, China.

the RCS in the end-fire direction can be reduced by using flat corrugated slot line to replace exponential gradient curve on both sides of the antenna [17]. In Reference [18], a half-mode substrate integrated waveguide (HMSIW) structure is first utilized to design the low RCS Vivaldi antenna. In view of reference [18], a novel SIW structure is designed to obtain the RCS reduction in a wider frequency band [19]. Nevertheless, there are few analyses on controlling the bistatic RCS in [19]. Based on the previous work [19], a low RCS bilateral Vivaldi antenna utilizing the substrate integrated waveguide (SIW) structure is proposed. Different from [19], the focus of this paper is paid on the flow direction of electromagnetic energy and analyses the bistatic RCS reduction as well as reducing the monostatic RCS. The RCS reduction of the antenna is achieved almost covering the whole operation frequency band. And more importantly, the electromagnetic energy can be led to the low threating direction by using the guiding effect of SIW on energy.

SIW and HWSIW have been the subjects of intense investigation for years [20–22], and many devices have been proposed using SIWs: filters [23, 24], antennas [25, 26], and power divider [27]. As a type of planar wave-guided structures, SIW has some unique advantages over rectangular waveguide, such as low profile, cheap processing cost and low loss. Besides, it can be easily integrated with the printed circuit board. Due to the SIWs with the oblique bending structure, the propagation of electromagnetic wave flows to the lateral side of antenna plane, thus the forward and backward RCS can be reduced.

The antenna design is introduced in Section 2. For comparison, a traditional bilateral Vivaldi antenna is chosen as the reference antenna, with the same dimension as the designed antenna. Section 3 presents the simulation and mechanism of RCS reduction, including three parts: radiation performance, monostatic RCS and bistatic RCS. Conclusions are outlined in Section 4. Both the reference and proposed antennas are fabricated and measured, and all the simulation works are made by using Ansoft's High Frequency Solution Solver (HFSS) software.

2. ANTENNA DESIGN

Figure 1 shows the geometry of the reference and proposed antennas. The antenna is designed on two pieces of substrates, which is Rogers 5880 with relative dielectric constant of 2.2 and a thickness of 0.5 mm. A stripline with an impedance of 50 Ω is employed to excite the bilateral Vivaldi antenna. Two SIWs with the width of $W1$ are formed by the four rows of the metallic via-holes and two pieces of metallic patches on the two sides of the substrate. The first and last row of the metallic via-holes and the two pieces of metallic patches form two HMSIWs with the width of $W2$. In order to guide the scattering energy to the lateral side, four rows of oblique via-holes are introduced with an oblique angle of 45°, as shown in Fig. 1(b). The reference antenna has the same geometry with the proposed antenna except the via-holes structure.

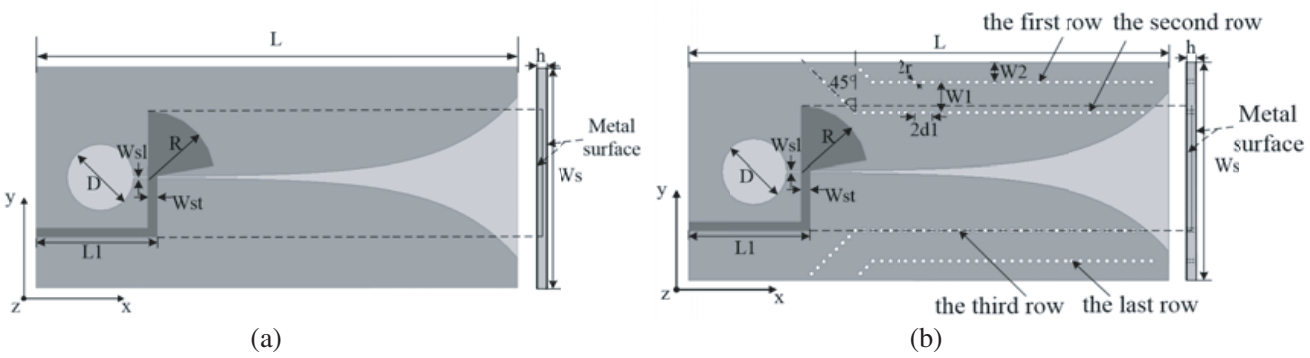

Figure 1. Geometry of (a) the reference antenna and (b) the proposed antenna.

More in detail, the parameters of the proposed antenna are presented in Table 1. The positions and widths of the SIWs in Fig. 1(b) are optimized to preserve the ideal radiation property and realize the outstanding RCS reduction in a wider band. Besides, the radius (r) and space ($d1$) of the metal via-holes satisfy the equation: $d1/(2 * r) < 3$ [28].

Table 1. Parameters of the reference and proposed antenna.

Parameters	D	R	Wsl	Wst	r	$d1$
Value (mm)	6	6	0.2	0.8	0.2	0.8
Parameters	Ws	$W1$	$W2$	L	$L1$	h
Value (mm)	20	2.8	1.8	44	11.1	1

3. SIMULATED AND MEASURED RESULTS

3.1. Radiation Performance

To verify the proposed strategy, the prototypes of the reference and proposed antennas are fabricated and measured, and the photographs are displayed in Fig. 2. In detail, Fig. 2(a) is the top side of the design and Fig. 2(b) is the bottom side.

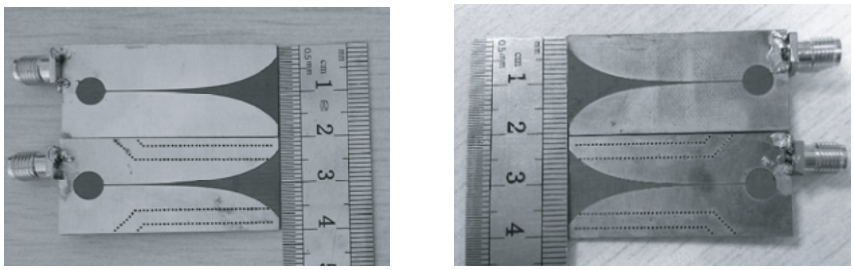

(a) (b)

Figure 2. (a) Top side and (b) bottom side of the fabricated antennas.

The reflection coefficient and gain curves versus frequency of the reference and proposed antennas are depicted in Fig. 3. It can be obviously seen that this design has a very little impact on the reflection coefficient and the gain almost remains unchanged compared with the reference one. From Fig. 3(a), the measured results of the two antennas are slightly higher than the simulated results. This is mainly due to the fabrication tolerance, material errors and measurement uncertainty. What's more, the maximum gain loss in the radiation direction (x-axis) is 0.29 dB, which is mainly due to the existence of holes on the radiation patch.

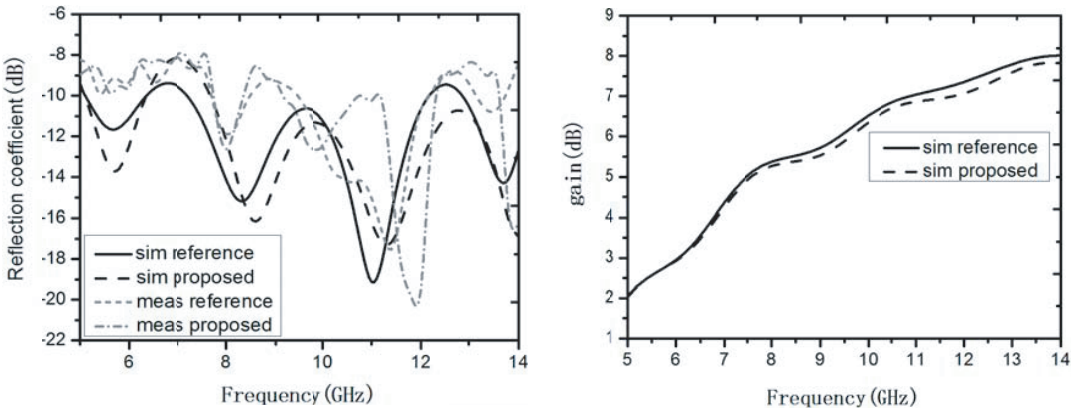

(a) (b)

Figure 3. (a) Reflection coefficient and (b) gain of the reference and proposed antenna.

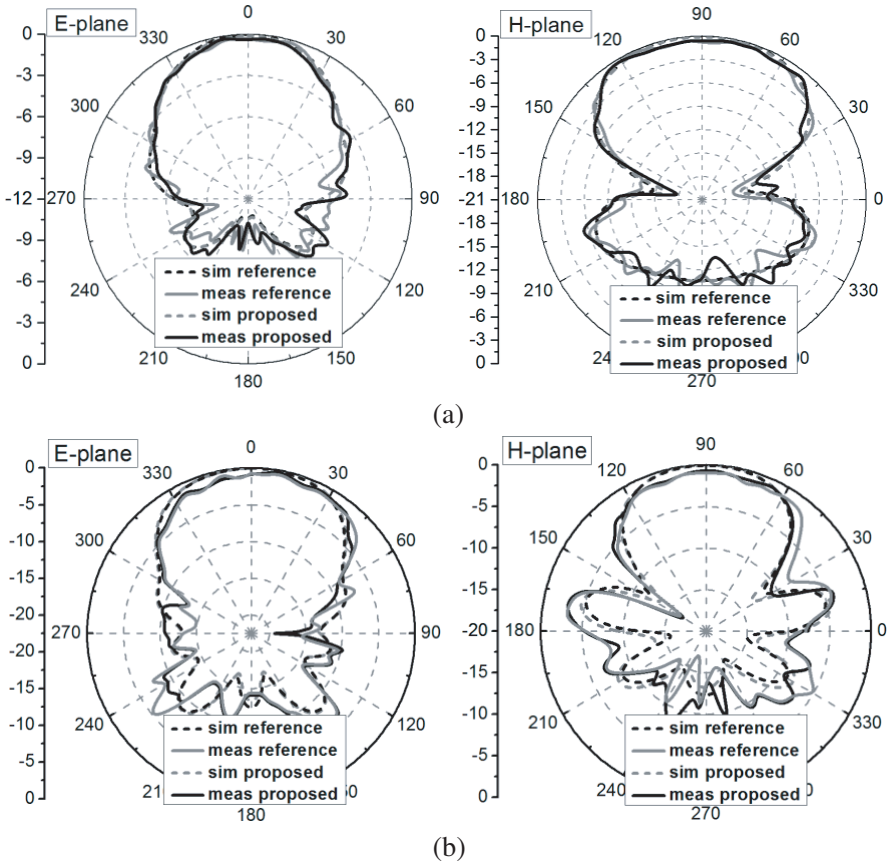

Figure 4. Simulated and measured radiation patterns at (a) 7 GHz and (b) 12 GHz in E- and H-plane.

The simulated and measured radiation patterns at 7 GHz and 12 GHz are shown in Fig. 4. From the radiation patterns at different frequencies, one can conclude that the radiation patterns of the proposed antenna are almost the same as the reference antenna. In detail, the maximum gain loss between the simulated and measured results is 0.83 dB, and it is also because of the fabrication tolerance and measurement error. In a word, the utilization of the SIWs does not affect the radiation characteristics and the impendence matching of the antenna.

3.2. Monostatic Radar Cross Section

Experiments and simulations have proved that dispersion characteristics of the SIW are the same as those of its equivalent rectangular waveguide [28]. The equivalent width of the SIW with a very good approximate equation is proposed in [28]. Because the SIW has similar performance as the conventional rectangular waveguides, the SIW with different widths can be excited at different frequencies. As a result, the proposed antenna with various widths of SIW and HMSIW realizes the wideband RCS reduction.

The monostatic RCS comparisons between the reference and proposed antenna irradiated by θ-polarized (vertical polarization) plane wave are exhibited in Fig. 5. As shown in Fig. 5(a) with the incident angle of $\theta = 90°$, $\varphi = 0°$, the RCS of the proposed antenna is reduced dramatically over a wide frequency band ranging from 5 GHz to 12 GHz, and the maximum reduction is as much as 34.73 dB compared with that of the reference antenna. When $\theta = 80°$ as Fig. 5(b) shows, the electromagnetic energy guided by the SIWs is reduced with the decrease of the incidence angle, thus the RCS reduction is not as noticeable as when $\theta = 90°$. This phenomenon testifies that the SIWs are the main contribution to the reduction of the RCS. In addition, the approach is ineffective for the φ-polarized (horizontal polarization) plane wave, because TM modes cannot be excited in the SIW [28].

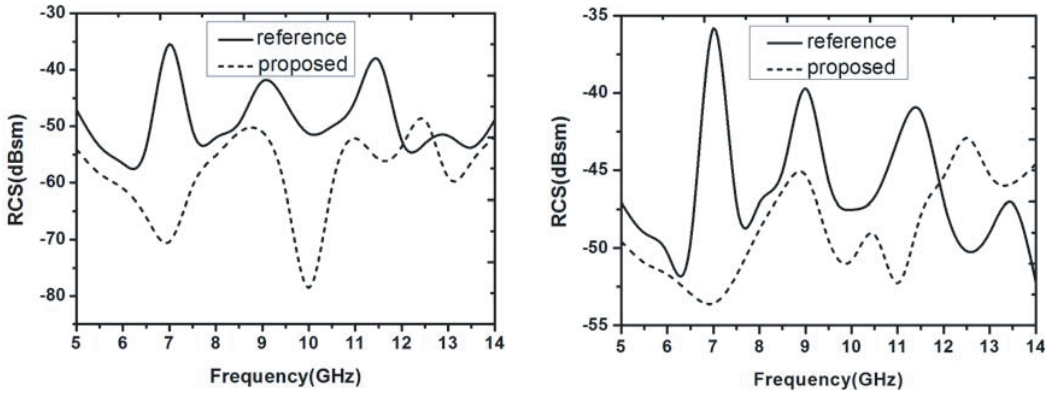

Figure 5. Comparisons of monostatic RCS between the reference and proposed antenna with the incident angles of (a) $\theta = 90°$, $\varphi = 0°$ and (b) $\theta = 80°$, $\varphi = 0°$.

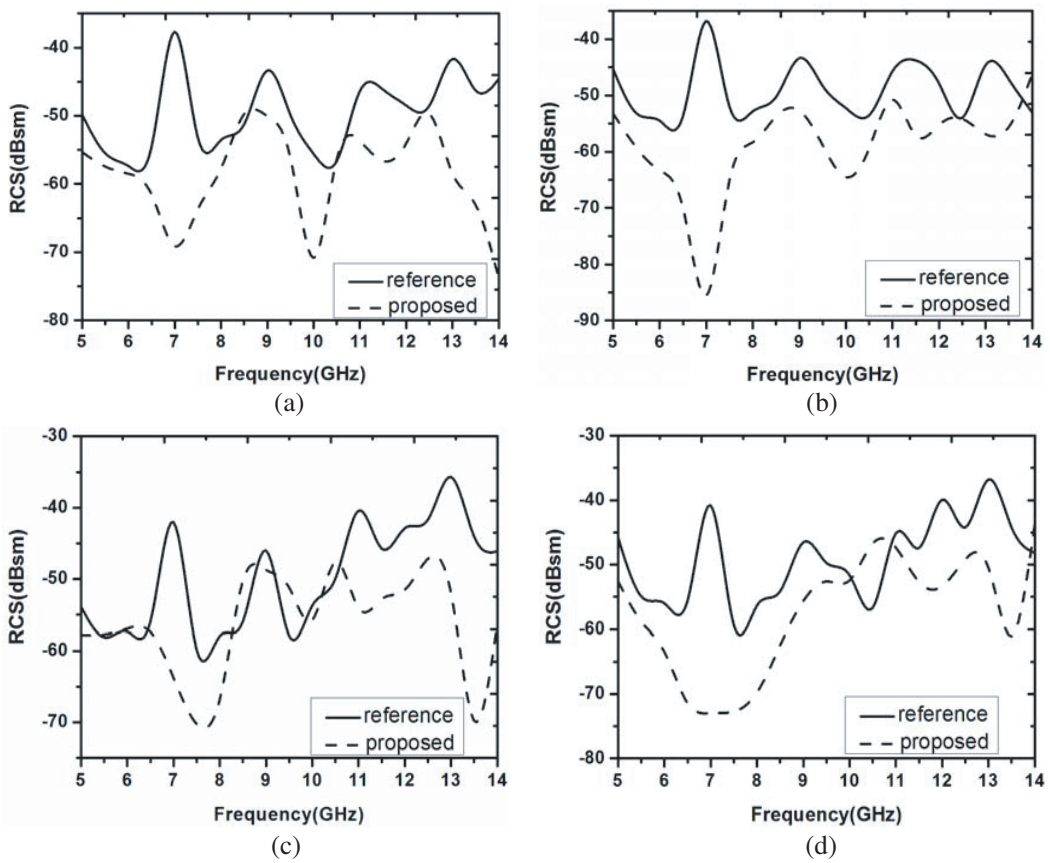

Figure 6. Monostatic RCS curves for θ-polarized plane wave with the incident angles of (a) $\varphi = 15°$, $\theta = 90°$, (b) $\varphi = -15°$, $\theta = 90°$, (c) $\varphi = 30°$, $\theta = 90°$ and (d) $\varphi = -30°$, $\theta = 90°$.

The monostatic RCS for θ-polarized (vertical polarization) plane wave, with the incident angles of $\varphi = \pm 15°$, $\pm 30°$ and $\theta = 90°$, are also simulated. As shown in Fig. 6, the monostatic RCS of proposed antenna is reduced dramatically. It indicates that the novel design has a stable property of the monostatic RCS reduction over a certain angle range.

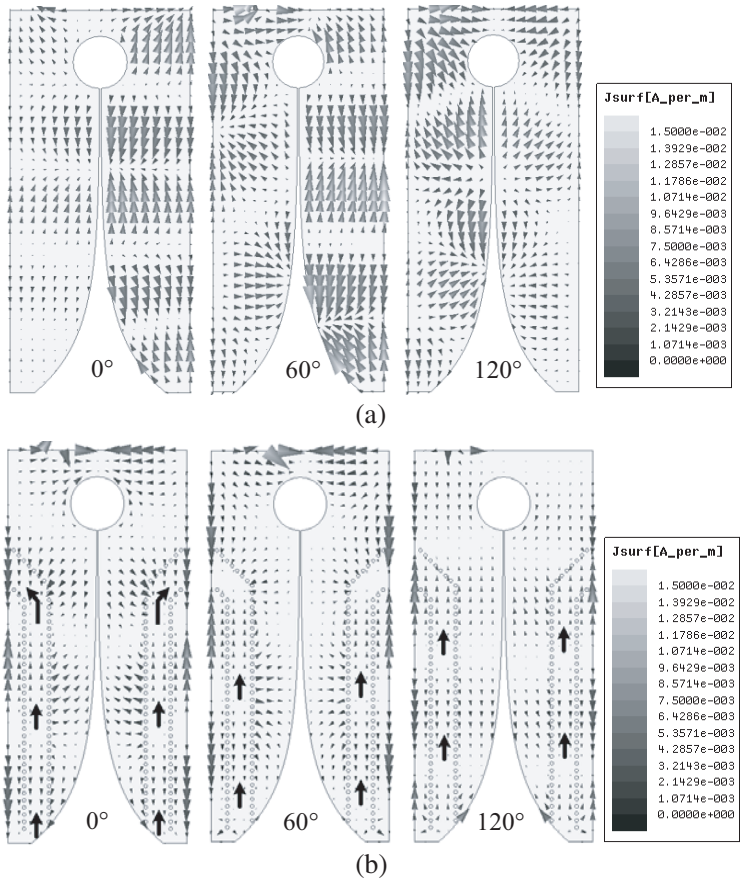

Figure 7. Surface current distributions of 0°, 60° and 120° at 12 GHz.

3.3. Bistatic Radar Cross Section

The surface current distributions of the reference and proposed antenna, which are irradiated by the θ-polarized plane wave at 12 GHz and 6 GHz are illustrated in Fig. 7 and Fig. 8 respectively. Moreover, the incident angles are $\varphi = 0°$ and $\theta = 90°$. The phases of surface current distribution are 0°, 60° and 120°, respectively. It is obvious that the incident plane wave will excite the SIWs in this case. As is apparent from Fig. 7(b), the energy flows in the SIWs with the variation of the phase, and the electromagnetic energy is led to the lateral side of antenna plane due to the wave-guiding characteristics of SIWs. Nevertheless, the energy distribution near the edge of the reference antenna does not change obviously, as shown in Fig. 7(a). Besides, the electric field intensity of the proposed antenna is smaller than that of the reference antenna. Thus, the monostatic RCS of the proposed antenna is reduced, and the bistatic RCS in the lateral side of the proposed antenna will increase compared with that of the reference antenna.

At low frequency, the incident plane wave will excite the SIWs with wider width. As shown in Fig. 1(b), two SIWs with the narrower width ($W1$) are formed by the four rows of the metallic via-holes and two pieces of metallic patches. A wider quasi SIW is generated by the second and third row of the metallic via-holes, and the metallic patches of quasi SIW are etched continuous gradual change slot-line. Certainly, the transmission characteristic of the quasi SIW is damaged because of the slot on the metallic patches, but the guided-wave property doesn't completely disappear. From Fig. 8(b), the quasi SIW transmits the energy with the variation of the phase.

The bistatic RCS in the xoy-plane varies with φ ranging from 0° to 360°, emphatically analysed in this paper. The regions of $\varphi = 45°$ to 135° and $\varphi = 225°$ to 315° are defined as region2, and $\varphi = 135°$ to 225° are defined as region1, shown in Fig. 9. On account of the wave-guiding characteristic of the SIWs, the oblique structures of the SIWs will lead the energy to the lateral side of the antenna (region2).

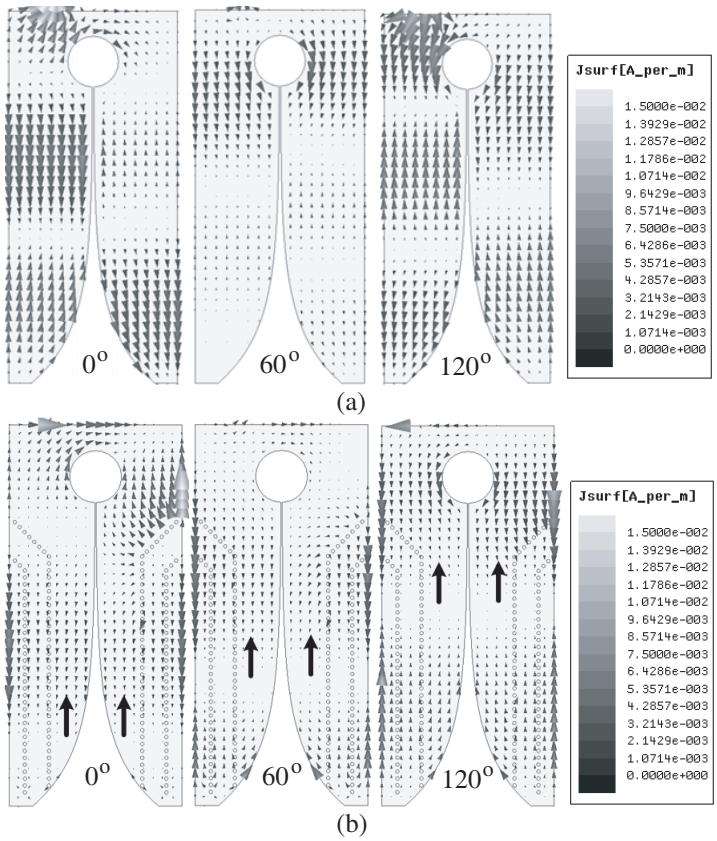

Figure 8. Surface current distributions of (a) reference antenna and (b) proposed antenna with the phase of 0°, 60° and 120° at 6 GHz.

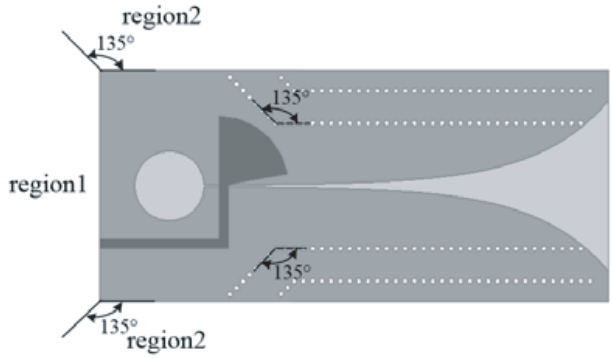

Figure 9. Sketch map of antenna zoning.

To prove the validity of the above analysis, the bistatic RCS comparisons between the reference and proposed antenna are presented in Fig. 10. It is emphasized that the incident plane wave is θ-polarized with the incident angles of $\varphi = 0°$ and $\theta = 90°$. Furthermore, the observed frequencies are 5.8 GHz and 8.9 GHz.

Compared with the reference antenna, the proposed antenna leads the scattering energy to the lateral side. Thus the forward and backward RCS are reduced, while the lateral RCS (region2) is increased. Consequently, it can be concluded that the wave-guiding characteristic of SIWs is able to be widely utilized for leading the propagation orientation of scattering energy to the low threat angular domain in the application of bistatic RCS control.

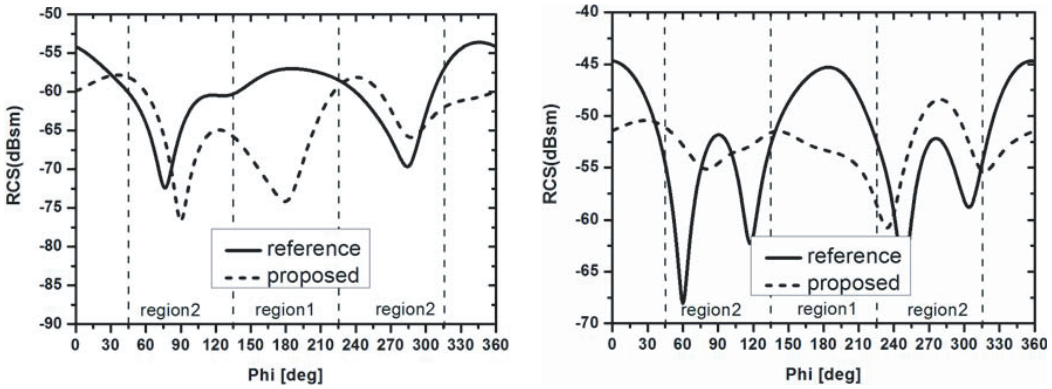

Figure 10. Bistatic RCS of reference and proposed antenna at (a) 5.8 GHz and (b) 8.9 GHz in *xoy*-plane.

4. CONCLUSION

A novel design has been developed for RCS reduction of Vivaldi antennas. Due to the guiding role of SIW with oblique bending structure, the bistatic RCS is controlled, and the scattering energy can be guided away from the threat direction. Thus, an outstanding wideband RCS reduction from 5–12 GHz is achieved under the premise of preserving the radiation performance. Moreover, the analysis and simulation have demonstrated that the SIW can be widely applied to design a bilateral Vivaldi antenna with low RCS.

ACKNOWLEDGMENT

This work was supported by the National Basic Research Program of China-973 program 2015CB857100, National Natural Science Foundation of China (Nos. 61401327, 61471278, 61601350), the Foundation of Chinese Academy of Space Technology (CAST 2015-11), and Natural Science Basic Research Plan in Shaanxi Province of China (No. 2015JQ6217).

REFERENCES

1. Knott, E. F., J. F. Shaeffer, and M. T. Tuley, *Radar Cross Section*, IET Digital Library, 2004.
2. Chen, T., W. X. Li, Z. H. Yao, X.-X. He, and X. Wang, "A novel stealth Vivaldi antenna," *Proceedings of International Conference on Microwave and Millimeter Wave Technology*, 1–4, May 2012.
3. Dikmen, C. M., S. Cimen, and G. Cakir, "Planar octagonal-shaped UWB antenna with reduced radar cross section," *IEEE Trans. Antennas and Propag.*, Vol. 62, No. 6, 2946–2953, Jun. 2014.
4. Wang, F. W., W. Jiang, T. Hong, H. Xue, S.-X. Gong, and Y.-Q. Zhang, "Radar cross section reduction of wideband antenna with a novel wideband radar absorbing materials," *IET Microw. Antennas and Propag.*, Vol. 8, No. 7, 491–497, May 2014.
5. Costa, F., S. Genovesi, and A. Monorchio, "A frequency selective absorbing ground plane for low-RCS microstrip antenna arrays," *Progress In Electromagnetics Research*, Vol. 126, 317–332, 2012.
6. Turpin, J. P., P. E. Sieber, and D. H. Werner, "Absorbing ground planes for reducing planar antenna radar cross-section based on frequency selective surfaces," *IEEE Antennas Wireless Propag. Lett.*, Vol. 12, 1456–1459, 2013.
7. Xu, S. and Y.-M. Xu, "Research on active cancelation stealth technique," *Optik-International Journal for Light and Electron Optics*, Vol. 125, No. 20, 6219-6222, Oct. 2014.
8. Singh, H. and R. M. Jha, "Active radar cross section reduction: Theory and applications," *Teaching Sociology*, Vol. 39, No. 3, 274–289, Mar. 2015.

9. Xiang, Y. C., C. W. Qu, F. Su, and M.-J. Yang, "Active cancellation stealth analysis of warship for LFM radar," *Proceedings of the 10th International Conference on Signal Processing*, 2109–2112, Oct. 2010.
10. Liu, Y., K. Li, Y. T. Jia, Y.-W. Hao, S.-X. Gong, and Y. J. Guo, "Wideband RCS reduction of a slot array antenna using polarization conversion metasurfaces," *IEEE Trans. Antennas and Propag.*, Vol. 64, No. 1, 326–331, Jan. 2016.
11. Jia, Y. T., Y. Liu, Y. J. Guo, K. Li, and S.-X. Gong, "Broadband polarization rotation reflective surfaces and their application on RCS reduction," *IEEE Trans. Antennas and Propag.*, Vol. 64, No. 1, 179–188, Jan. 2016.
12. Gibson, P. J., "The Vivaldi aerial," *Proceedings of the 9th European Microwave Conference*, 101–105, Sept. 1979.
13. Schaubert, D. H., S. Kasturi, and A. O. Boryssenko, "Vivaldi antenna arrays for wide bandwidth and electronic scanning," *Proceedings of the 2nd European Conference on Antennas and propagation*, 1–6, Nov. 2007.
14. Liu, J. F., S.-X. Gong, Y. X. Xu, and X.-L. Zhang, "Study of RCS on the dual-index Vivaldi antenna," *Space Electronic Technology*, 26–29, 2011.
15. Zhang, G. Q., L.-M. Xu, and A.-X. Chen, "RCS reduction of Vivaldi antenna array using a PSS boundary," *Proceedings of the 8th International Symposium on Antenna, Propagation and EM Theory*, 345–347, Nov. 2008.
16. Jiang, W., Y.-P. Li, S.-X. Gong, and W. Wang, "Novel UWB Vivaldi antenna with low RCS," *Proceedings of Asia-Pacific Microwave Conference*, 1405–1407, Nov. 2014.
17. Luo, T. and Z. P. Nie, "RCS reduction of antipodal Vivaldi antenna," *Proceedings of Asia-Pacific Microwave Conference*, 1–3, Dec. 2015.
18. Jia, Y. T., Y. Liu, Y.-W. Hao, and S.-X. Gong, "Vivaldi antenna with reduced RCS using half-mode substrate integrated waveguide," *IET Electron. Lett.*, Vol. 50, No. 5, 345–346, Feb. 2014.
19. Jiang, W., J. J. Xue, and L. Yang, "Novel design for RCS reduction of Vivaldi antenna," *Proceeding of the 4th Asia-Pacific Conference on Antennas and Propagation*, 608–609, Jun. 2015.
20. Deslandes, D. and K. Wu, "Integrated microstrip and rectangular waveguide in planar form," *IEEE Microw. Wirel. Compon. Lett.*, Vol. 11, No. 2, 68–70, Feb. 2001.
21. Hong, W., B. Liu, Y. Q. Wang, Q.-H. Lai, H.-J. Tang, X.-X. Yin, Y.-D. Dong, Y. Zhang, and K. Wu, "Half mode substrate integrated waveguide: A new guided wave structure for microwave and millimeter wave application," *Proceeding of the 31st International Conference on Infrared Millimeter Waves and the 14th International Conference on Terahertz Electronics*, 219–219, Sept. 2006.
22. Grigoropoulos, N., B. Sanz-Izquierdo, and P. R. Young, "Substrate integrated folded waveguides (SIFW) and filters," *IEEE Microw. Wirel. Compon. Lett.*, Vol. 15, No. 12, 829–831, Dec. 2005.
23. Coq, M. L., E. Rius, J. F. Favennec, C. Quendo, B. Potelon, L. Estagerie, P. Moroni, B. Bonnet, and A. E. Mostrah, "Miniaturized C-band SIW filters using high-permittivity ceramic substrates," *IEEE Trans. Compon. Packag. Manuf. Technol.*, Vol. 5, No. 5, 620–626, May 2015.
24. Pourghorban Saghati, A., A. Pourghorban Saghati, and K. Entesari, "Ultra-miniature SIW cavity resonators and filters," *IEEE Trans. Microw. Theory Tech.*, Vol. 63, No. 12, 1–12, Dec. 2015.
25. Tan, L. R., R. X. Wu, and P. Yin, "Magnetically reconfigurable SIW antenna with tunable frequencies and polarizations," *IEEE Trans. Antennas and Propag.*, Vol. 63, No. 6, 2772–2776, Jun. 2015.
26. Guan, D. F., C. Ding, Z.-P. Qian, Y.-S. Zhang, W.-Q. Cao, and E. Dutkiewicz, "An SIW based large-scale corporate-feed array antenna," *IEEE Trans. Antennas and Propag.*, Vol. 63, No. 7, 2969–2976, Jul. 2015.
27. Li, G. L., K. J. Song, F. Zhang, and Y. Zhu, "Novel four-way multilayer SIW power divider with slot coupling structure," *IEEE Microw. Wirel. Compon. Lett.*, Vol. 25, No. 12, 799–801, Dec. 2015.
28. Xu, F. and K. Wu, "Guided-wave and leakage characteristics of substrate integrated waveguide," *IEEE Trans. Microw. Theory Tech.*, Vol. 53, No. 1, 66–73, Jan. 2005.